Stanford 3D PAC Technical Report
2025

Lawton Skaling
Mark Tian

Acronyms

3DPAC - 3D Printed Aircraft Competition
AOA - Angle of Attack
BEC - Battery Eliminator Circuit
CA Glue - Cyanoacrylate Glue (More commonly known as super glue)
CAD - Computer Aided Design
Cd - Coefficient of Drag
Cl - Coefficient of Lift
Cm - Pitching Moment Coefficient
ELRS - ExpressLRS (High Performance Open Source Radio Control Link)
ESC - Electronic Speed Control
FDM - Fused Deposition Modeling
LW-PLA - Light Weight Polylactic Acid
MAC - Mean Aerodynamic Chord
NACA - National Advisory Committee for Aeronautics
NASA - National Aeronautics and Space Administration
PLA - Polylactic Acid
RC - Radio Control
SAE - Society of Automotive Engineers
XFLR - Computational Tool Used for Aerodynamic Analysis

Coordinate Systems

In this report, the aircraft will use the standard **SAE/NASA** body-fixed coordinate system. This is defined with the +Z direction pointed down, +X forward on the body, and +Y defined as the cross product of the two.

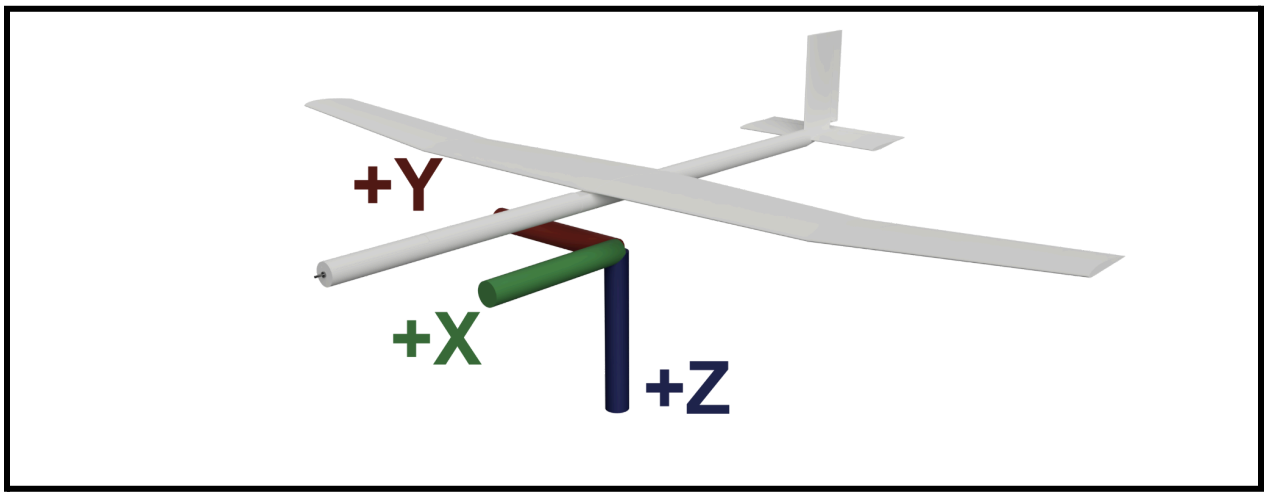

Figure 1. Aircraft coordinate system

The report will also use the convention for 3D printer axes,+X moves the nozzle to the right, +Y moves the bed away from the user interface, and +Z raises the nozzle upward from the build

plate.

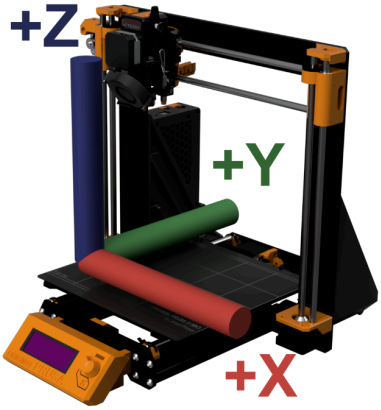

Figure 2. 3D Printer coordinate system

Team Information

Figure 3 and 4. Lawton Skaling (Left), Mark Tian (Right)

Lawton Skaling is a Senior at Stanford University studying Mechanical Engineering. He competed in the UT Arlington 3D printed plane competition in 2022 and is excited to restart the project. He has been flying RC planes since elementary school and was president of Stanford Flight Club in 2023. He's also a 3D printer enthusiast and enjoys merging theory and application to create optimized structures within the constraints of additive manufacturing processes.

Pengxiang(Mark) Tian is a freshman at Stanford University planning to major in Electrical Engineering. He is fascinated by the world of 3D printing and is a self admitted 3D printing nerd! From beginning with modifying Ender 3 Pros, to designing his own 3D printers he loves how additive manufacturing allows him to express his imagination. Mark also loves the world of aerospace, and has built and designed 3D printed airplanes before. He is excited to tackle the 3DPAC competition for the first time!

1. Aircraft Design

Our aircraft is unique as we centered our design around manufacturability. Early on, we identified weight to be the greatest factor to improve the performance of the aircraft. Weight reduces induced drag, meaning more efficient flying and longer glide time. It also reduces the energy of impact, which most of the load cases are based on. We put extensive effort into optimizing our design and manufacturing process to optimize aircraft mass.

To do this, we developed a novel 3D printing technique that our analysis showed significantly increases the strength to weight ratio of structural components. The wing is printed horizontally on the build plate (wing -Z aligned with printer +Z), and the fuselage is printed in half with the split on the build plate (fuselage +/-Y aligned with printer +Z). Doing this requires compromises to be made to the aerodynamics to enable fabrication, however allows far thinner airfoil covers, stronger parts that are designed around FDM printing's inherent anisotropy, and assembly optimizations such as built-in hinges and aerodynamic covers.

In designing our aircraft around manufacturability, our analysis was conducted in reverse of many student teams. Typically a design goes from aerodynamic analysis to structural analysis, manufacturing analysis, and then prototyping. We started with a prototype as we identified our manufacturing process to be our greatest risk early on, and then moved into manufacturing analysis to identify how the manufacturing process constrains the aircraft, and finally conducted an aerodynamic and structural analysis together to optimize the remaining design space. We've done this through two iterations, and by the competition will be flying our third aircraft iteration.

We have been iteratively developing the aircraft through a series of prototypes, relentlessly pushing the manufacturability of the aircraft to reduce assembly time during each iteration while optimizing the performance. We have over 30 minutes of flight time to date on the aircraft and expect to have an order of magnitude more by competition.

1.1 Configuration and *CAD*

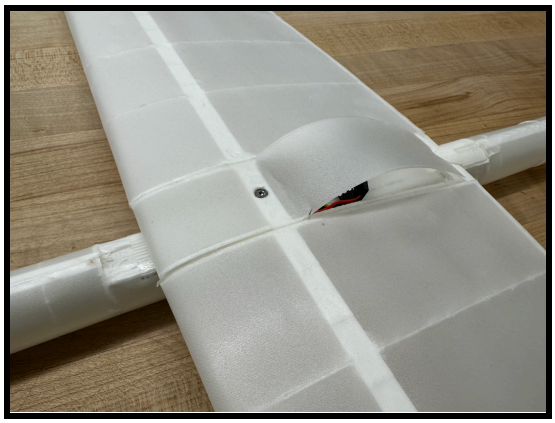

Our aircraft has a 1.4m wingspan, and weighs 340g. One of our constraints was to design the aircraft to be transportable across campus to our flying site and to the competition by car. This requires the wing to be detachable from the fuselage. We opted for a high wing aircraft for improved roll stability and simplified assembly. It assembles using an M3 screw to fasten the wing, a 3D printed slot to guide alignment, and a cover in the center of the airfoil to access servo connectors.

We opted for a traditional empennage design as it's more efficient than a V-tail, and easier to ship than a T-tail. Furthermore, we chose a puller motor configuration for improved aerodynamics, as the motor can be mounted axially with the fuselage, minimizing the aircraft's cross section. The fuselage is a 30mm diameter tube, consistent across the length. Keeping a consistent geometry simplifies manufacturing and improves aerodynamics.

The aircraft is four channel, with independent aileron control for easier trimming. Servos and servo wires are embedded in the wing and the fuselage, reducing drag.

Component	Actual weight (g)	Percent	CG about wing leading edge (mm)	Moment about wing leading edge (mm * g)
Vertical stabilizer + aft fuselage	22.2	6.53%	-550	-12210
Rear aeroshell	1.5	0.44%	-620	-930
Horizontal stabilizer	19.2	5.65%	-620	-11904
Fuselage boom aft	8.5	2.50%	-187	-1589.5
Fuselage boom mid	8.5	2.50%	53	450.5
Fuselage boom front	8.5	2.50%	293	2490.5
Motor + propeller	41.5	12.21%	413	17139.5
Battery + ESC + BEC	30	8.83%	350	10500
Wing structure	160	47.07%	-60	-9600
Wing servos	20	5.88%	-80	-1600
Empennage servos	20	5.88%	-550	-11000
Total	**339.9**	**100.00%**		**-53.70108856**

Table 1. Mass breakdown

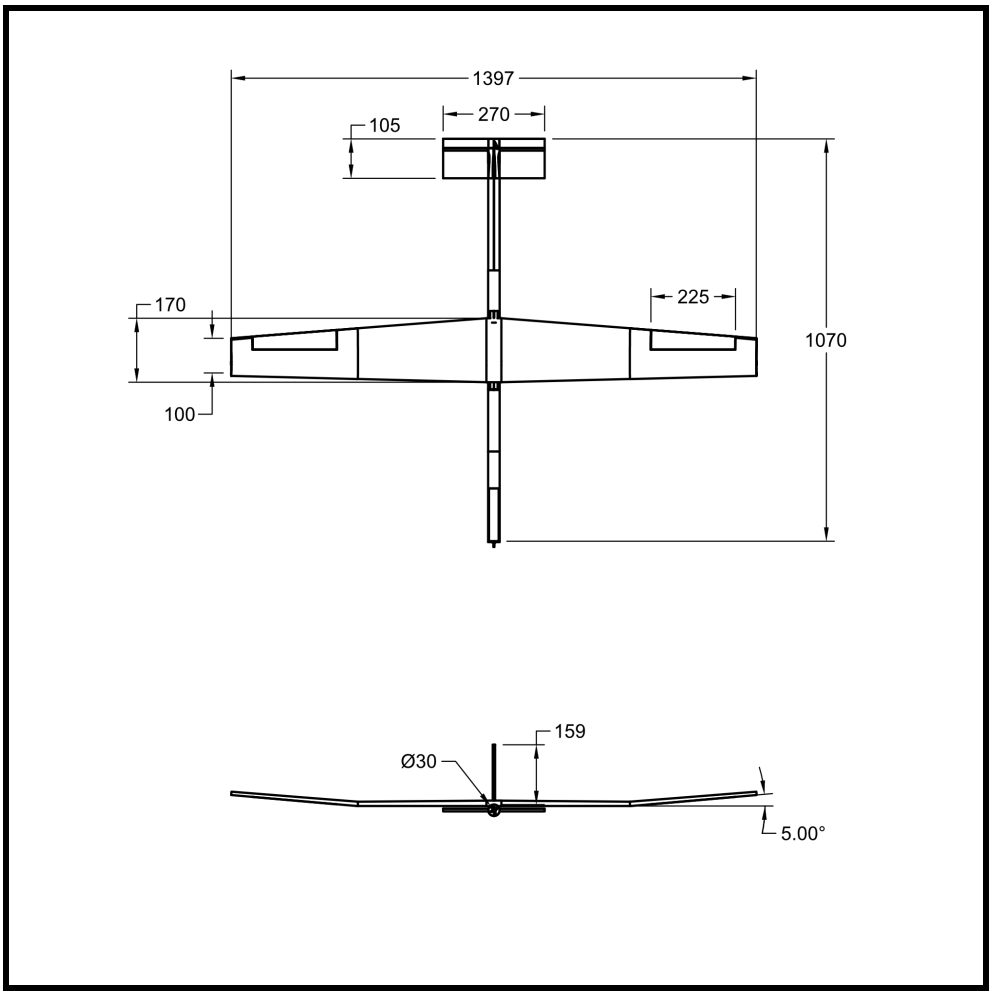

Figure 5. Aircraft dimensions (mm)

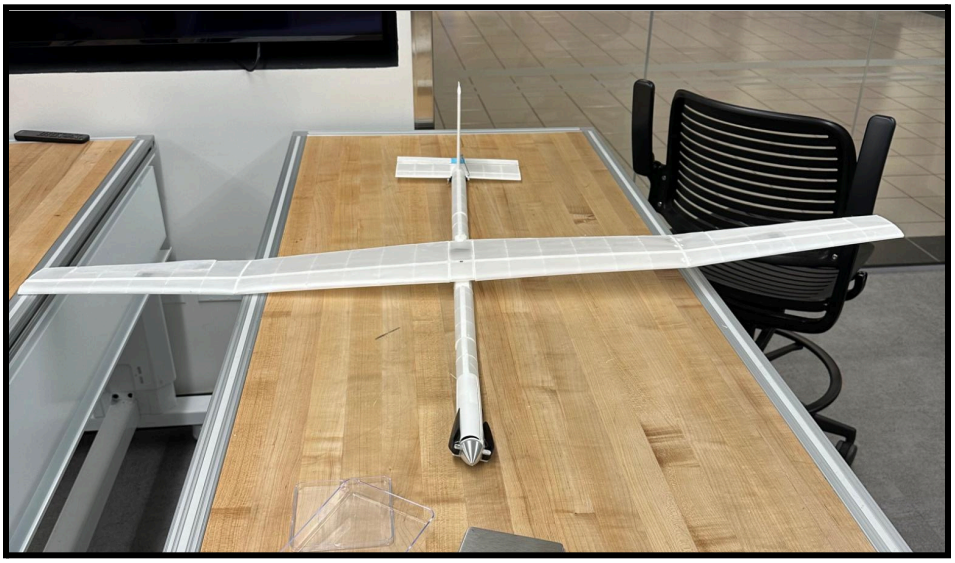

Figure 6. Prototype aircraft

1.2 Aerodynamic Analysis

The aircraft uses an N-9 airfoil for the wing. It has a root chord of 170mm and tip chord of 100mm, and is 1400mm long. The empennage leading edge is 540mm from the wing leading edge, and uses a *NACA* 008 airfoil for the horizontal and vertical stabilizers. The horizontal stabilizer is angled down 4º.

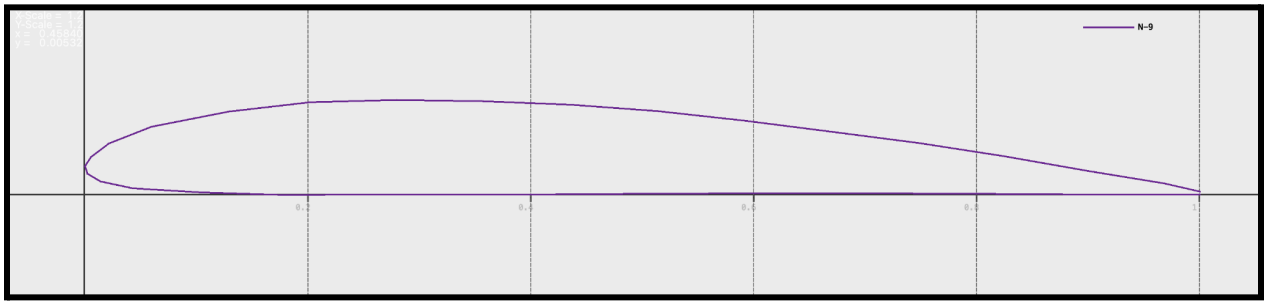

Figure 7. N-9 Airfoil

Aerodynamic analysis was performed in *XFLR 5* and a custom Python script. The primary focus of the aerodynamic analysis was determining the optimal airfoil and wing dimensions. To simplify analysis, we assumed the aircraft is gliding at a starting height of 35 ft, and optimized the time to reach the ground.

Airfoil constraints were defined by the manufacturing process. The airfoil must have a flat bottom to be printable in the configuration described in section 2.3, can be printed in no more than 360mm sections due to 3D printer build volume limits.

First, a survey of airfoils were conducted which yielded the following airfoils that fit the manufacturing constraints:

- Fage & Collins 1
- N-9
- N-22
- Dormoy
- AG35

Each airfoil was simulated at a variety of Reynolds numbers and *AOA* on *XFLR 5*. A first pass suggested the Reynolds number at the MAC of the wing would be 50,000. The point of highest *Cl/Cd* at any angle of attack was identified at this Re for each airfoil, which resulted in the N-9 airfoil being selected at a desired *AOA* of 4 degrees. It also exhibited better stall characteristics, with a good margin between ideal flight AOA and stall AOA.

Next, a variety of wing areas were simulated. These varied from 100mm root chord to 300mm in 50mm increments, and tip tapering to 66% of the root chord. All were simulated 1.4m in length, as that was estimated to be the longest before aeroelastic effects, shipping costs, and max operable windspeed would drive design criteria. The aircraft was iteratively simulated at different

flight speeds until the airfoil generated the lift required to overcome the assumed weight of the aircraft (300g for the thinnest wing, 400g for the widest). The highest *Cl/Cd* at any *AOA* was selected to compare.

Finally, all this data was fed into a Python script which would use the *Cl/Cd* and velocity to determine the time aloft. While earlier analysis approximated the most efficient flight as operating at max *Cl/Cd* the ideal flight would operate slightly above, as the max *Cl/Cd* optimizes for glide distance and the *3D PAC* competition challenges glide time. This python script simulated that, producing a theoretical glide time.

1.3 Stability and Control Analysis

The control surfaces were sized to create a maneuverable, highly inherently stable aircraft. One of the tradeoffs of a high camber wing that we selected is it creates a pitching moment that the horizontal stabilizer must counteract.

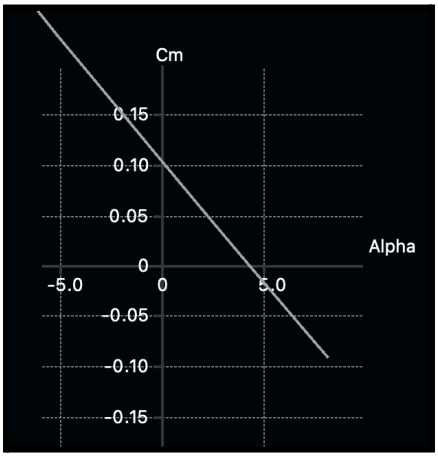

The horizontal stabilizer was sized iteratively in *XFLR 5* to obtain a highly stable pitch aircraft that flies with a neutral *AOA* at the aircraft's optimal glide angle. Analysis at varying horizontal stabilizer angles was performed to determine when the *Cm* vs *Alpha(AOA)* intercept suggested a neutral *AOA* of 4 degrees, and a slope of $-\ 1.4\ rad^{-1}$.

The vertical stabilizer was sized using the following equation:

$$V_v = (S_v * l_v)/(S * b)$$

Where S_v is the vertical stabilizer area, l_v is the distance from the wing to the vertical stabilizer, S is the wing area, and b is the wingspan.

We targeted 0.025 as is standard for *RC* gliders, giving an area of $17\ cm^3$

A 5 degree dihedral was added to the outer 25% of the wing to improve roll stability. Aeroelastic effects also add a small amount of dihedral to the wing further improving roll stability.

1.4 Propulsion / Power

Our propulsion system was designed to reach up to 60 ft in 8 seconds, as required by the UT Arlington competition. We developed a first pass estimate of power requirements by assuming a 20% efficiency at converting power to lift, and a 300g aircraft. This was validated with flight testing to be an underestimate of the actual power required.

$$PE = mgh = 0.3 * 9.81 * 20 = 59\ J$$
$$E = PE\ /\ (efficiency * time) = 59\ /\ (0.2 * 8) = 94.4W$$

We selected the Dualsky XM2221EG-22 2900KV motor as it provides a maximum of 126W, giving a good margin from the calculations, weights only 30g, has a mounting geometry

favorable for reducing the gap between the propeller cap and fuselage, and uses a 3mm unthreaded shaft which is compatible with most folding propellers.

We selected folding propellers as the aircraft is unpowered for the majority of the flight, and folding propellers minimize drag during unpowered periods, furthermore the aircraft is not power constrained, so a small amount of efficiency loss during powered flight is acceptable. The propeller was chosen based on manufacturer recommendations for the motor, and validated during flight testing.

1.5 Electronics

The aircraft used off the shelf electronics mainly from pre-existing parts the Stanford Flight Club already owned. We utilized a FrSky RX6R 2.4G radio receiver, alongside a FrSky Taranis Q X7 that the Flight Club had available. The team looked into other radio protocols like *ELRS*, but found that it added increased complexity, extra cost, and no negligible reduction in weight. After analyzing commercially available *ESC*s with inbuilt *BEC*s, we realized that we would get significant weight savings from using a standalone *ESC* with an external *BEC*. The team settled on the lightweight Readytosky 35A *ESC* alongside the tiny Matek Micro *BEC*. After analyzing commercially available electric motors, we initially set upon repurposing quadcopter motors due to incredible power density and wide availability, but we found that the world of discus launched gliders had motors that better suited our purposes. So the team settled on using the Dualsky XM2221EG-22 2900kv due to the motor's incredible thrust to weight ratio, and ability to provide the necessary power for our glider design. The team also extensively researched the possibility of reusing quadcopter flight controller stacks(flight controller + electronic speed controller), due to the surprising compactness and mass of such systems. Ultimately the flight controller added unnecessary extra complexity, and made a negligible change in weight. The team utilized 2 gram servos due to their low weight and known reliability. For the battery, we selected the Tattu 300mAh 2S HV battery, as it was the smallest size that we found with 2 cells, and can discharge a maximum of 194W.

1.6 Structures

The major structural loads the aircraft is designed around two load cases:

- L1: -Z point load at the tip of the wing due to wing strike on landing
- L2: -Z point load at the rear of the fuselage due to impact on landing

Furthermore, to minimize aeroelastic effects, deformation under usual flight loads were analyzed for the following load cases:

- D1: -Z distributed load along the length of the wing
- D2: +/- X torsion on the aircraft fuselage due to aircraft roll and propeller torque

For the first three loading scenarios, an I-beam is desirable to maximize the second moment of area. For the last scenario, a hollow circular profile is ideal for maximizing the polar moment of inertia. To achieve this, an I beam is embedded in the wing at the maximum thickness point to

maximize the second moment of area. In the analysis, the spar is the load carrying member and the ribs and skin are not modeled.

For the fuselage, a similar I-beam is designed into the fuselage, maximizing the second moment of inertia for L2. The skin reacts the torsion to minimize rotation from D2.

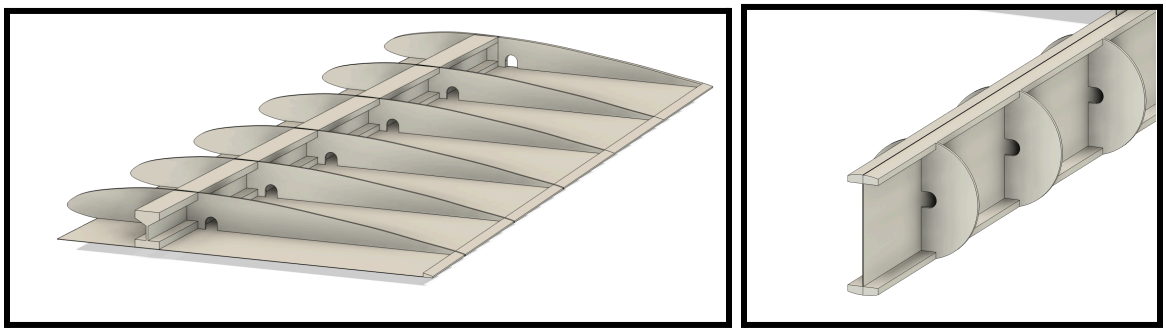

Figure 8/9. Aircraft section views.

The design was further optimized by utilizing our 3D printers multi material capability. *Section 2.1* shows that ColorFabb *LW-PLA* has the lowest density, however *PLA* has the highest specific strength. As the airfoil carries almost no load and the volume constraint is around printability, it's advantageous to be as light as possible. Meanwhile the spar should be as rigid as possible to satisfy D1, and as strong as possible to satisfy L1. We are able to satisfy both of these constraints by utilizing the printer's dual extruders to print both materials.

2. Manufacturing

2.1 Material Testing

The specific strength of the material we print our plane with was determined to be one of the highest leverage variables to reduce mass, so we put extensive effort towards testing and validating possible materials. Existing data for lightweight materials is incomplete and not standardized, requiring us to conduct our own tests.

We tested a variety of lightweight and standard filaments in tension. Due to concerns of the sun's radiative heating causing the aircraft to become more elastic or permanently deform during the competition, only white filaments were tested, ruling out carbon fiber composite filaments. All filaments were printed with manufacturer recommended settings. They were printed on Bambu Lab 3D printers with full perimeters and a slow print setting. During testing, force was applied parallel to the walls of the sample on the tensile test and bending force was applied perpendicular to the printing plane. In both cases this represents the strongest orientation of the part, and the loading direction the plastic will experience stress during flight.

We began with a survey of 3D printer materials, purchased the best options, and tested it using an Intron tensile tester. We tested both tension and bending, with the results of tensile testing

shown below. Note that the elasticity measurements are approximate as the machine was not equipped with an extensometer to measure the displacement of the sample, however it's believed any error scales proportional to the force, meaning the relative elasticities are accurate.

Filament	Measured density (g/cm^3)	Tensile strength (MPa)	Specific tensile strength (kN·m kg^{-1})	Tensile modulus (MPa)
Recreus PLA-LW	0.840	5.833	6.941	0.603
ColorFabb LW-PLA	0.553	4.167	7.532	0.414
ASA-Aero	0.521	4.167	7.993	0.298
Overture Air PLA	0.872	7.500	8.598	0.894
PLA	1.213	23.333	19.240	2.164
PETG	1.202	16.667	13.864	1.244

Table 2. Density and strength of printed samples

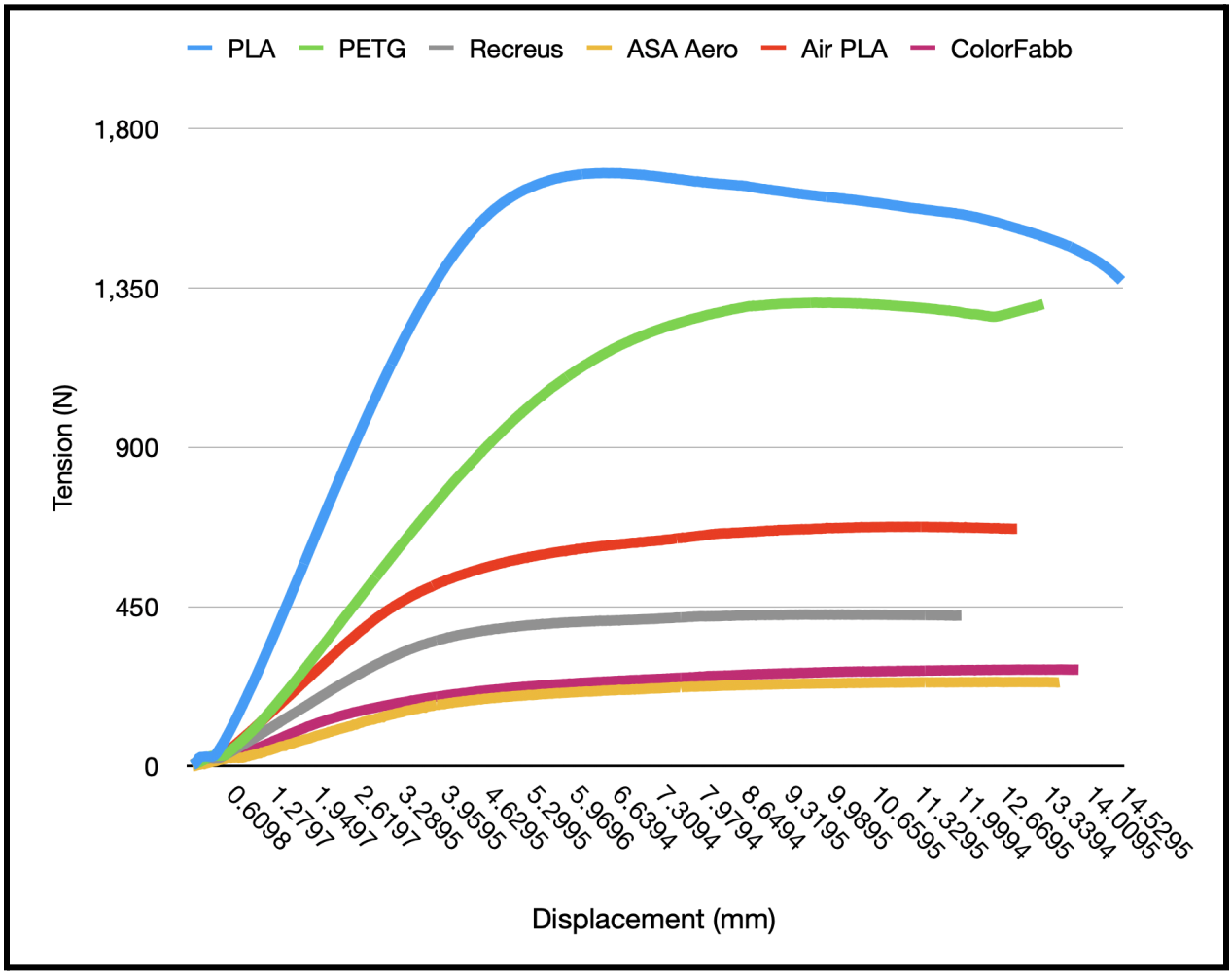

Figure 10. Stress strain curves of printed samples

Figure 11. Printed samples.

2.2 Processes and Technologies

We have access to the following printers at public makerspaces on campus and at Stanford Flight Club's workspace

Printer	Build Volume	Technology	Notes and constraints
Prusa XL	360mm x 360mm x 360mm	Multi-toolhead *FDM*	Has multi-material capability
Prusa 3.5, 3.9, 4.0	250mm x 210mm x 210mm	*FDM*	Only limited to one filament type
BambuLab X1C	254mm x 254mm x 254mm	Multi-Material Management System *FDM*	Cannot print different types of filaments together

Table 3. Printers available on campus

We decided to print most components on the Prusa XL, as the large build volume reduces the complexity of assembly, and the multi-material printing is useful for combining lightweight and

standard filament as described in section 1.6. Smaller components like the horizontal stabilizer or control surfaces were printed on Prusa 3 printers and the BambuLab X1C.

2.3 Design for Manufacturing

Nearly all parts of the aircraft are printed without support. The fuselage is printed in halves such that each half doesn't require support. The airfoil has a flat bottom to print flat without support, and the horizontal stabilizer is printed in halves to produce a symmetric airfoil.

The "skin film" is modeled as a flat 0.16mm body. In the slicer the first layer is tuned to the minimum we found would consistently print without voids where the bed leveling causes under extrusion, which is also 0.16mm. Choosing to make the film attach to the structure improves assembly accuracy compared to printing as a separate sheet.

The ribs of the structure are constrained by the minimum wall thickness of the printer - 0.8mm to allow for two perimeters on the interior ribs. The outside ribs are printed at 2mm to give sufficient contact area for the skin film

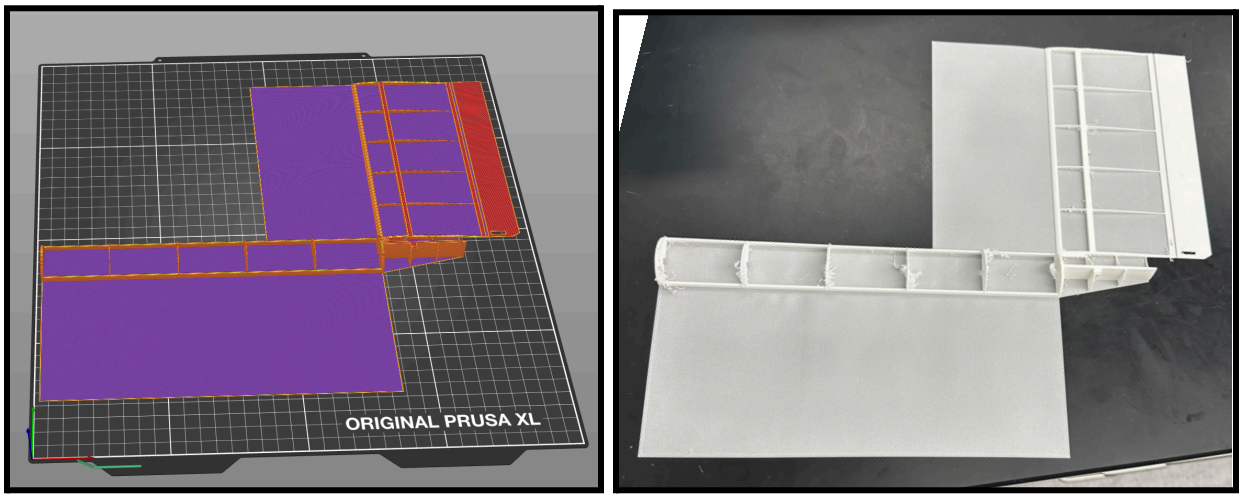

Figure 12. Slicer and print model

2.3 Assembly

After printing, each part is post processed to remove stringing caused by the LW-PLA foaming. CA glue is used to bond parts together. Servos are first installed so that the wires can route through the fuselage and wing. The skin film is then folded, bonded, trimmed, and then sections of the wings and fuselage are bonded together.

Hinges are similarly constructed using the thin film technique, with a single layer of plastic acting as a hinge. This improves the aesthetics and alignment of control surfaces compared to a tape

hinge. To further reduce drag, a thin film is printed on the bottom of the ailerons, leaving no gap when the aileron is undeflected while allowing a smooth transition in a downward deflected aileron.

In the final assembly, wires are trimmed to length and crimped, pushrod and horns are added to the control surfaces, and the motor is installed.

Figure 13/14. Aircraft empennage, wing servo and control surface

3. Innovations, Lessons Learned, Observations

Stanford Flight Club is excited to participate in the 3D printed RC Plane Competitions. Our thesis in pursuing this project was:

- Manufacturing optimizations should be at the forefront of the design process and drive the aerodynamic and structural analysis
- Reducing mass is the highest leverage way to improve glide time of the aircraft
- Iteratively designing the aircraft is crucial to testing and improving the design, which can only be accomplished with smart manufacturing techniques to minimize manufacturing time

Neither member of our team has an aerospace background, so we've spent the past months learning aerodynamic analysis by first principles and aided by tools like XFLR 5, with extensive testing to validate our methods. We've also applied skills from our disciplines, particularly with manufacturing to ensure a printable aircraft, and incorporating ways to improve assembly like adding alignment features and building fixtures.

Over the past four months we've kept our tenets in mind as we developed our aircraft. From the start we optimized the design to use FDM 3D printing's anisotropic nature to our advantage, and focused our structural and aerodynamic analysis around it. We've developed three iterations of our aircraft and have extensively flight tested each to see how our analysis compares to the actual flight, practice flying as we will in competition, and test the structural limits of the aircraft. We're excited to share what we've been working on!